

Hole trapping in carbon nanotube-polymer composite organic light emitting diodes

H. S. Woo[†]

Wooyoung Institute of Technology, Seoul, Korea 136-791

R. Czerw, and D. L. Carroll

Department of Physics and Astronomy, Clemson University,
Clemson SC 29634

Abstract

Controlling carrier transport in light emitting polymers is extremely important for their efficient use in organic opto-electronic devices [1]. Here we show that the interactions between single wall carbon nanotubes (SWNTs) and conjugated polymers can be used to modify the overall mobility of charge carriers within nanotube-polymer nanocomposites. By using a unique, double emitting-organic light emitting diodes (DE-OLEDs) structure, we have characterized the hole transport within electroluminescent nanocomposites (nanotubes in poly (*m*-phenylene vinylene-co-2,5-dioctoxy-*p*-phenylene) or PmPV). We have shown using this idea that single devices with color tunability can be fabricated. It is seen that SWNTs in PmPV are responsible for hole trapping, leading to shifts in the emission wavelengths. Our results could lead to improved organic optical amplifiers, semiconducting devices, and displays.

Introduction

Within the last year there has been an explosion of interest in the properties of well dispersed nanomaterials in polymeric hosts, termed "nanocomposites"[2-4]. Of particular interest has been phenomena related to dispersions of carbon nanotubes in an organic matrix. When used in organic composites, their unique properties promise greatly enhanced strength, enhanced or modified thermal and electrical transport, and unusual optical nonlinearities [5]. To realize any of these properties enhancements for applications we must first have a detailed understanding of the

interactions between the carbon nanotubes and the local polymer environment. Ago *et. al.* proposed hole collecting properties of multiwall carbon nanotube from a conjugated polymer at the polymer composite region [6]. We have found recently that the SWNTs in a polymer matrix trap holes injected from anode in organic light emitting diodes (OLEDs) [7]. The redistribution of the trapped charges near highest occupied molecular orbital (HOMO) of the host polymer is followed by the introduction of discrete traps near the HOMO. This leads us to apply the hole trapping behavior of SWNTs in an emissive conjugated polymer on DE-OLEDs to control the hole mobility in a polymer composite layer, thus changing emission color. OLEDs based on conjugated polymers are one of the strong candidates in a flat panel display (FPD) due to the easy fabrication with high brightness. These conjugated polymers show a semiconducting behavior resulting from the delocalization of electrons and overlapping of P_z orbitals along the chain, thus opening the energy gap at the Fermi surface. Electrons and holes injected into the polymeric material through the cathode and anode, respectively, disturb and relax the polymer chains followed by formation of a neutral excitation, exciton. The light emission in OLEDs is due to a radiative recombination of the exciton. The challenges using polymer composite in OLEDs are not only the controlling the emission colors in multi-layered devices but also the improved device life time and possibly higher efficiency due to the capability of heat sink of the carbon nanotube and controlled charge injection, respectively [7, 8].

[†]Corresponding author

Tel : +82-2-961-3552~3, Fax : +82-2-961-3554

Email : hwoo@wooyoung.co.kr

Experimental

In this study, the transport behavior in a number of different conjugated systems will be described but we will focus primarily on the nanocomposite material fabricated from the emissive polymer, PmPV, and SWNT. A detailed description and analysis of the Horner synthesis route used for our PmPV is described elsewhere, however this polymer, shown in figure 1, has a *meta*-linkage added to allow for the formation of a coiled molecular conformation with a *cis-to-trans* ratio of approximately 30 % [9]. When combined with SWNT, this coiling has been shown to result in enhanced solubility of the tubes in the polymer, making it particularly nice for thin film fabrication. The SWNT used were arc grown and purified through the multistep filtration procedure reported by others [10]. The composite formed between these two materials appears clear with nanotube loadings up to a weight percent and shows no discernable aggregation. Composites with nanotube concentrations of 0.02, 0.05 and 0.1 wt.% were prepared through the ultrasonic dispersion of purified SWNT in chloroform followed by blending it with PmPV solution (7.5mg of PmPV in 1cc chloroform).

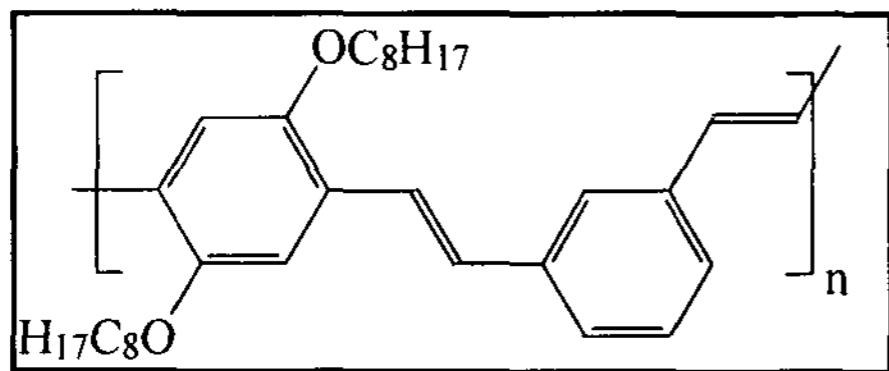


Figure 1. Molecular structure of PmPV

The devices used to investigate transport properties are based on a standard multi-layered structure, which allows work function matching between organics and contacts as shown in figure 2. This DE-OLED structure consists of a layer of polyethylene dioxythiophene - polystyrenesulfonate (PEDOT:PSS) from Bayer which acts as a buffer between the indium-tin-oxide (ITO) anode and the hole transport layer (HTL) or the emissive layer. On the buffer layer is put down, two emissive layers; first, the nanocomposite of PmPV and nanotubes, and the second, Nile Red doped Alq₃, an electron conducting emissive polymer. Pure PmPV and Nile Red doped Alq₃ devices were also prepared to allow a comparison between the electroluminescence (EL) spectra with those of the DE-OLEDs. In pure Nile Red doped Alq₃

device, vacuum evaporated N,N'-diphenyl-N,N'-bis(3-methylphenyl)1-1'-biphenyl 1-4,4'-diamine (TPD) with thickness of 20 nm was used for a HTL between the buffer and emitting layers.

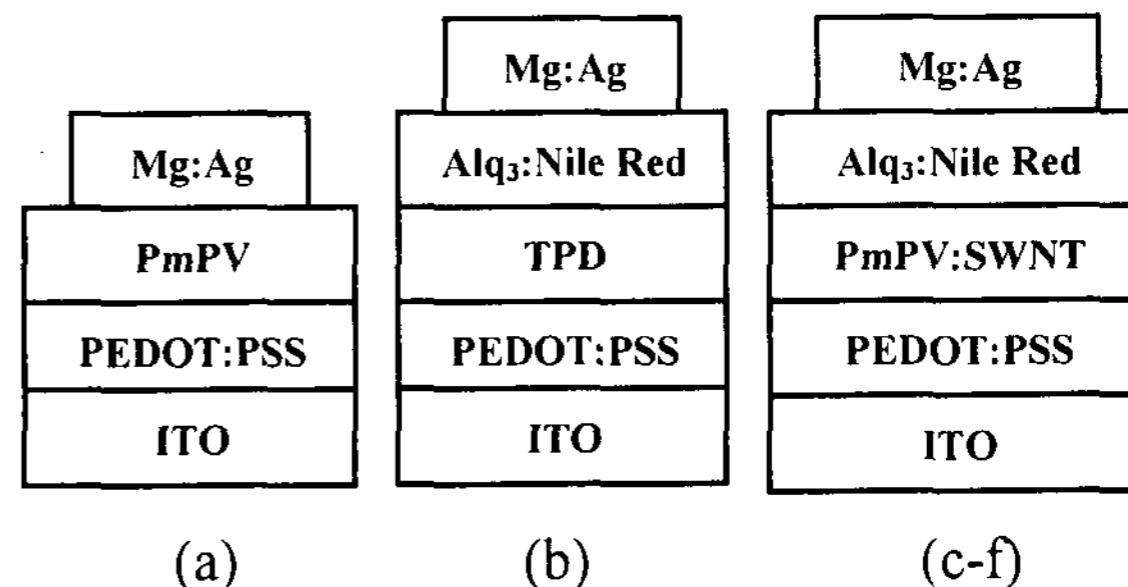


Figure 2. Schematic diagram of the OLEDs. Note that the device (c) is pure PmPV without SWNTs.

For the fabrication of our devices, PEDOT:PSS and PmPV composites were spun with spin speed of 5000 and 1500 rpm in ambient conditions, respectively, giving the film thickness of about 80 nm for both materials. The Alq₃ and Nile Red were vacuum co-evaporated with a film thickness of 20 nm, giving the Nile Red concentration of 1 wt. %. For all devices, Mg and Ag alloy with 10:1 wt. ratio was used as a cathode with a thickness of 200 nm. The evaporation rate of 0.1 nm/sec and 0.5 nm/sec with the evaporation pressure about 5×10^{-6} Torr were maintained during the depositions for organics and cathode metals, respectively. The device structures used in this study are summarized as follows:

device (a): anode / PmPV / Mg:Ag

device (b): anode / TPD / Alq₃:Nile Red / Mg:Ag

device (c): anode/PmPV/Alq₃:Nile Red / Mg:Ag

device (d): anode / PmPV:SWNT (0.02 wt. %) / Alq₃:Nile Red / Mg:Ag

device (e): anode / PmPV:SWNT (0.05 wt.%)

/Alq₃:Nile Red / Mg:Ag

device (f): anode/PmPV:SWNT (0.1 wt.%) / Alq₃:Nile Red / Mg:Ag

where, the anode denotes ITO/PEDOT:PSS and the doping concentrations of Nile Red in Alq₃ for the devices numbered from 2 to 6 are all same (1 wt. %). The forward current - voltage (I/V) characteristics and the EL spectra were measured with a source measurement unit (Keithly 236) and a luminescence spectrometer (Perkin Elmer LS-50B), respectively.

In the DE-OLED device, holes injected through the ITO must pass through the buffer layer, the hole transport layer and the emissive composite (PmPV-SWNT). Electrons injected at the cathode, move through the Alq₃ layer and meet the holes to form polaronic exciton which decay and release light. Generally speaking, in π -conjugated system, the holes are the "fast carriers" while electrons are slow. Therefore, without nanotubes, we expect, from the layer thicknesses used in the DE-OLED, for the holes and electrons to form a recombination region in the Alq₃, bypassing the PmPV. However, with the nanotubes in composite with the PmPV, striking alterations in the transport is observed with the recombination zone position dependent on the tube loading in the composite.

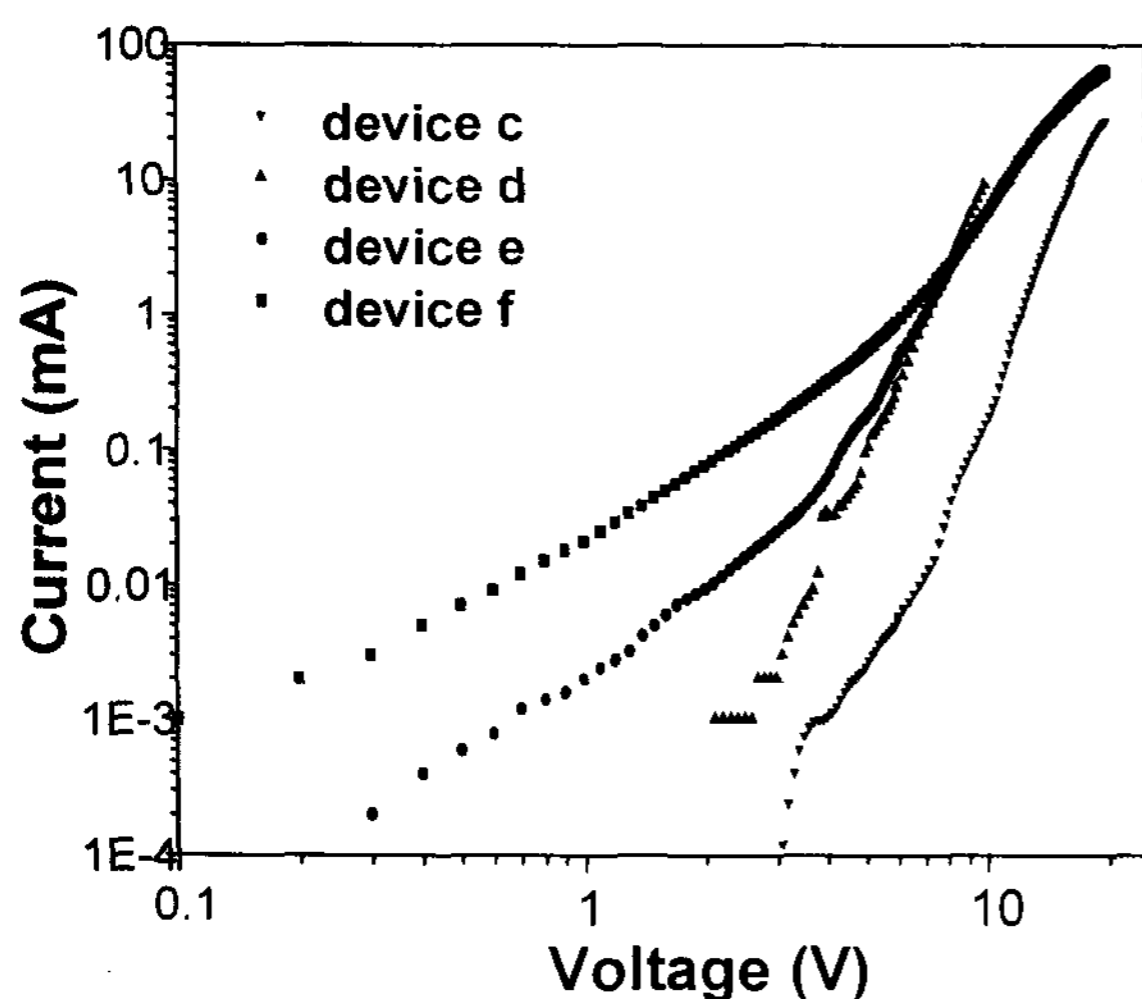


Figure 3. The I/V characteristics of ITO / PEDOT / PmPV:SWNT / Alq₃:Nile Red(1 wt.%) / Mg:Ag with a SWNTs concentration of devices (c) 0.0 %, (d) 0.02 %, (e) 0.05 %, and (f) 0.1 %.

The first indication that transport within the composite is dominated by the nanotube loading is seen in the current – voltage (I/V) response of the devices. The I/V characteristics of devices from (c) to (f) are shown in figure 3. Notice that for each case, a different I/V power law dependence is observed according to the SWNT concentration in the PmPV, for low voltages. At voltages less than 4 V, the device with the SWNT concentration of 0.1 wt. % for example, shows $I \sim V^2$ while the pure PmPV device has $I \sim V^5$. The later case is, of course, the continuous-trap charge limit (C-TCL) due to the structural or chemical defects within the polymer

chains and is well known [11], while the former, as we propose in this report, is a case of discrete-trap charge limit (D-TCL) that occurs due to discrete traps generated by the hole collecting SWNTs in the polymer composites. We note that the I/V characteristics of all the devices have nearly the same power law dependence ($I \sim V^2$), above applied biases of 20 V. This is clearly a case of the trap free space charge limit (SCL) with all the traps filled.

To understand this behavior, we can apply a simple transport model for the polymer layers, which includes a single discrete trapping state [12]. As shown below, the same power law dependence of the I/V, $J \sim V^2$, will be observed between the SCL and the discrete-trap charge limit (D-TCL) regimes with different magnitude of current for each. For the PmPV composite device with 0.1 wt. % of SWNTs, the hole mobility of $\mu = 1.3 \times 10^{-10} \text{ m}^2 / \text{Vs}$ is calculated from Fig. 3 and using Eq. (3) in ref. [13] in SCL regime with values of $J = 3.6 \times 10^3 \text{ A} / \text{m}^2$ at 20 V, $K = 3.5$, and $d = 10^{-7} \text{ m}$. Again from Fig. 3 and Eqs. (5) and (6) in ref. [13], with the assumption of a weak field dependence of mobility and a high trap density regime ($H_t \sim 10^{19} / \text{cm}^3$), the discrete trap energy of the same device was estimated as $E_t = 0.09 \text{ eV}$ relative to the HOMO of the PmPV composite with values of $H_{\text{HOMO}} \sim 10^{20} / \text{cm}^3$, and $J = 1.43 \text{ A} / \text{m}^2$ at 1 V. The same calculation gives $E_t = 0.27 \text{ eV}$ for the low trap density regime ($H_t \sim 10^{16} / \text{cm}^3$). Again, this result assumes of course the weak field-dependence of the mobility. This trap energy distribution is smaller than that of the binding energy of the excitations in the polymeric system, usually between 0.3 - 0.5 eV, or other structural defects which might be responsible to form the continuous traps. In fact, the mobility is expected to be smaller at lower bias. Thus the real value of the trap energy will be smaller than what we have obtained. Therefore, at low applied voltage, the injected holes fill the discrete traps prior to the continuous traps. This discrete trap filling can cause the hole blocking in the PmPV composite leading to a higher probability of balanced radiative recombination in the PmPV composite. However, as shown in Fig. 3, the slope of the I/V characteristics for the device with PmPV composite tends to increase as the bias increases, indicating that the device enters into the C-TCL regime as the discrete traps are filled. It is expected, at high bias voltage where the SCL conduction dominates, that the radiative recombination of all devices takes place in Nile Red doped Alq₃. With a bias voltage of 20 V, all the

devices emitted in the near-red. In the intermediate range of the applied voltage, 4 V - 10 V, the D-TCL and the C-TCL can co-exist in the PmPV composite devices leading to double emission features (one from the PmPV layer and another from the Nile Red doped Alq₃ layer). These emission characteristics are shown in figure 4.

From the EL spectra of the devices, numbered (c) to (f) in figure 4, the change in position of the recombination zone becomes evident. A forward bias of 7 V was applied to all of the devices. In order to compare the oscillator strengths of the green emissions, the EL spectra of the devices numbered (c) to (f) were normalized with the red emission peaks.

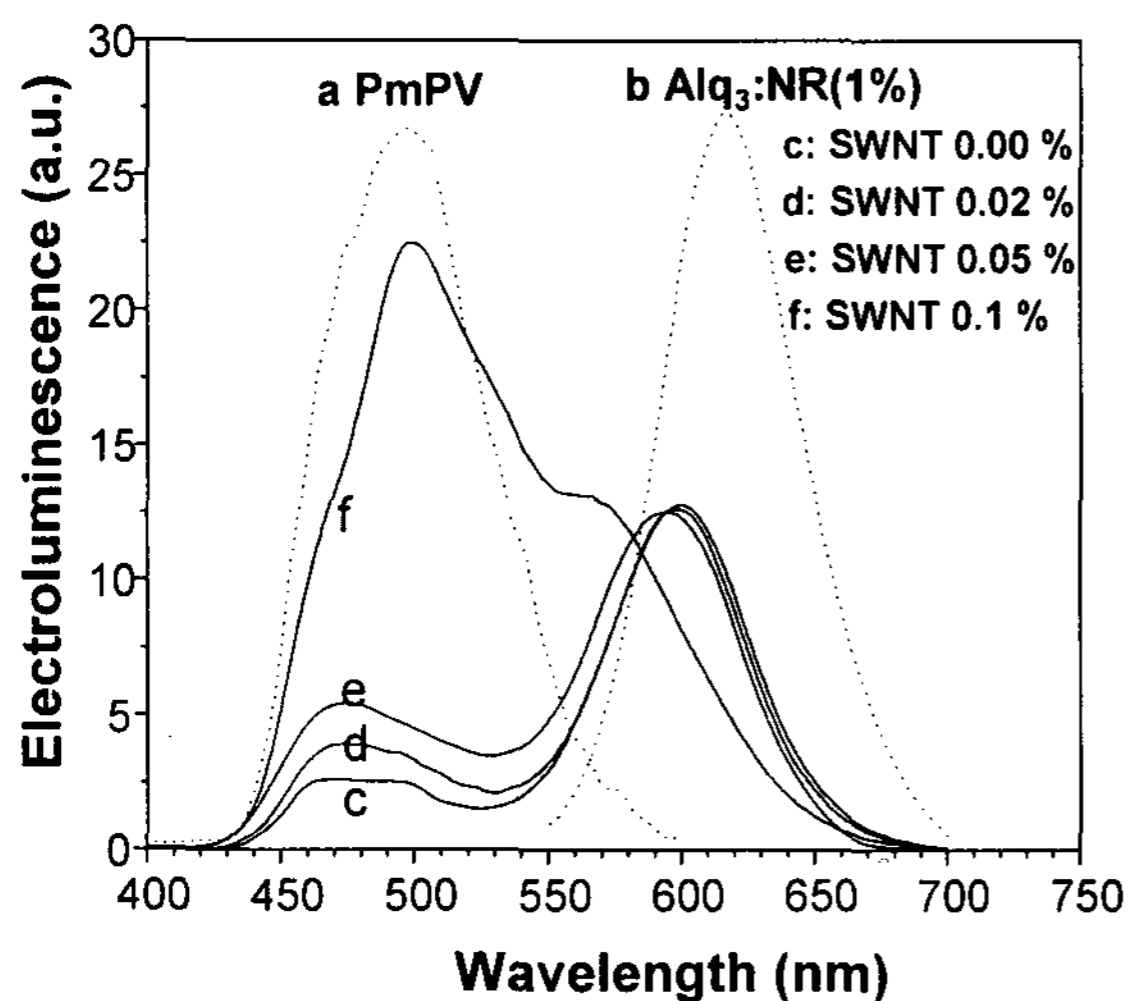


Figure 4. The normalized double emitting EL spectra of : device (c); device (d); device (e); and device (f) with those of the single emitting devices, (a) and (b)

In figure 4, the EL from the Nile-Red doped Alq₃ has a peak near 618 nm while the pure PmPV emits green with major peak at 500 nm with small vibronic features near 470 and 540 nm. It is clear that the device without SWNT in the PmPV (device c) emits near red at 600 nm, which is in the range of the characteristic emission of Nile Red in Alq₃, with a small contribution of 470 nm feature in PmPV. This indicates that the PmPV in the device (c) acts as a hole transport material so that most of the radiative recombination takes place in Alq₃:Nile Red layer. However, the devices fabricated with the PmPV composites show that the oscillator strength of the green emission increases as the nanotube concentration increases, with the shifting of the 600 nm feature to the blue. In device (f) with high SWNT

concentration (0.1 wt. %), a noticeable enhancement of green emission was observed with the shifting of its emission peak closer to 500 nm, the characteristic emission of pure PmPV. We note in device (f) that the large blue shift of the 600 nm feature is shown, its peak appearing near 560 nm. This implies that the SWNT in PmPV composites act as a hole blocking material, generating the hole traps in the PmPV composite, thus shifting the recombination regions from the doped Alq₃ layer to the PmPV composite layer. We also note that the EL of PmPV composite with SWNTs concentration of 0.1 % has same emission feature (500 nm) with that of pure PmPV, indicating the SWNT do not act as an exciton migration center in PmPV. As shown in figure 5, the trends in increasing green emission and the blue shifting of the red peaks, as the SWNTs concentration are increases, are very similar to each other, This is also an indication of a shifting of the recombination region from the doped Alq₃ layer to the PmPV composite layer.

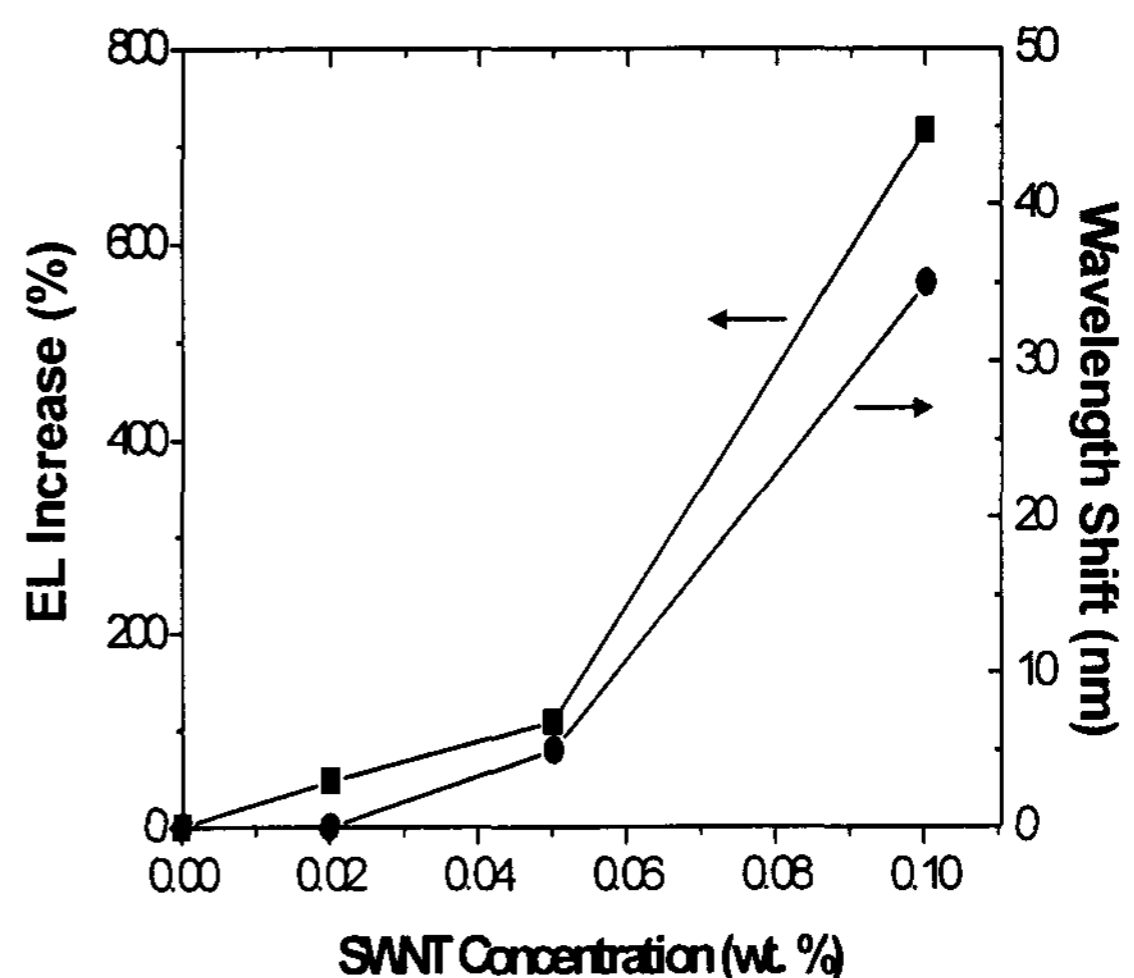


Figure 5. The % increase in an integrated oscillator strengths of the green emission and the blue shift of the red peaks relative to those of the 0 % of SWNTs, respectively, as a function of the SWNTs concentration

Result and Discussion

In conclusion, the I/V characteristics of the DE-OLEDs shows, at the low applied voltage (below 4 V), that the devices prepared with PmPV composites have a I/V power law dependence of $I \sim V^2$ while the one with pure PmPV has $I \sim V^5$. We propose that, in the former, the power law dependence of $I \sim V^2$ is due to the discrete-hole traps generated by the SWNT in the polymer matrix while the later is a case of the C-TCL

due to the structural or chemical defects in the PmPV composite. Using a single discrete trap approximation, the discrete trap energy was estimated to be in the range of 0.09 eV ~ 0.27 eV according to the trap density distribution, relative to the HOMO of the PmPV composite. This trap energy distribution is smaller than the binding energy of the structural defects or excitations in a polymeric system, which might be responsible to form the continuous traps. Thus, at low applied voltage, the injected holes fill the discrete traps prior to the continuous traps. This implies that the SWNT in PmPV is responsible for the blocking of the holes in the PmPV composite, forming a D-TCL regime in the polymer matrix, with no change in the binding energy of a singlet exciton or acting as an excitation migration center. This leads, as we demonstrated in the EL spectra, that the SWNTs in a PmPV shifts the radiative recombination region in our DE-OLEDs, from the Nile Red doped Alq₃ layer to the PmPV composite layer without changing the PmPV emission energy. This color tunability may help to realize the easy fabrication of full color OLEDs. In terms of the device reliability, the carbon nanotube in OLEDs could act as a heat sink with a creation of polymer-nanostructure matrix by wrapping the carbon nanotubes with polymer chains, thus increasing the device life time [8]. This morphology change also leads to modifying the electronic properties of the polymer composite which might be responsible to the hole traps. Our work leaves more study of polymer-nanostructured materials such as an electron trapping or transporting properties of the carbon nanotubes in polymer matrix. The more understanding of polymer-nanostructure properties will impact not only the pure scientific nature of this fascinating material but also the real applications based on the polymer composites. These applications are including OLEDs, solar energy conversion devices, optical fibers, and other opto-electronic devices as well as the applications based on electrically conducting polymers like electro-magnetic shielding materials, conducting wires, and rechargeable batteries.

Acknowledgements

The authors gratefully acknowledge funding from AFOSR. They also acknowledge Prof. Werner Blau at Trinity College in Dublin for providing the PmPV, Prof. P. M. Ajayan at Rensselaer Polytechnic Institute, and J. T. Morrison of Bayer for the PEDOT:PSS

References

- [1] T. Tsutsui, *MRS Bull.*, **22**, 39 (1997).
- [2] B. McCarthy, R. Czerw, D. Tekleab, A. Strevens, P. Iyer, P. M. Ajayan, W. J. Blau, and D. L. Carroll, (unpublished).
- [3] R. D. Antonov and A. T. Johnson, *Phys. Rev. Lett.* **83**, 3274 (1999).
- [4] H. Ago, K. Petritsh, M. S. P. Shaffer, A. H. Windle, and R. Friend, *Adv. Mater.* **11**, 1281 (1999).
- [5] R. Martel, T. Schmidt, H. R. Shea, T. Hertel, and Ph. Avouris, *Appl. Phys. Lett.* **73**, 2447 (1998).
- [6] H. Ago, M. S. P. Shaffer, D. S. Ginger, A. H. Windle, and R. H. Friend, *Phys. Rev. B*, **61**, 2286 (2000).
- [7] H. S. Woo, R. Czerw, S. Webster, D. L. Carroll, A. Strevens, D. O'Brien, and W. J. Blau, *Appl. Phys. Lett.* **77**, 1393 (2000).
- [8] S. A. Curran, P. M. Ajayan, W. J. Blau, D. L. Carroll, J. N. Coleman, A. B. Dalton, A. P. Davey, A. Dury, B. McCarthy, S. Maier, and A. Strevens, *Adv. Mater.* **10**, 1091 (1998).
- [9] A. P. Davey, A. Drury, S. Maier, H. J. Byrne, and W. J. Blau, *Synth. Met.* **103**, 2478 (1999).
- [10] T. W. Ebbesen and P. M. Ajayan, *Nature (London)* **358**, 220 (1992).
- [11] C. C. Wu, J. K. M. Chun, P. E. Burrows, J. C. Sturm, M. E. Thompson, S. R. Forrest, and R. A. Register, *Appl. Phys. Lett.* **66**, 653 (1995).
- [12] J. Yang, and J. Shen, *J. of Appl. Phys.* **84**, 2105 (1998).
- [13] We propose that the power law dependence of $I \sim V^2$ at the low applied bias (< 4 V) originates from a single discrete-hole trap generated by the SWNTs in the polymer matrix. To derive the effect of such traps, we begin with the ohmic conduction and Poisson equations with a single charge carrier approximation (ie. holes) in one-dimension, given respectively by:

$$J = h q \mu F \quad (1)$$

$$\partial F / \partial x = - (q / K \epsilon_0) (h + h_t) \quad (2)$$

where J is the current density, h and h_t are free and trapped hole concentrations, respectively, q is the electronic charge, μ is the hole mobility, F is the electric field strength, and $K\epsilon_0$ is the dielectric permittivity with the permittivity of vacuum ϵ_0 and the relative dielectric constant K . For the trap free or trap

29.1 / Plenary

filled SCL ($h_t = 0$), the solution to Eqs. (1) and (2) is known as the Child's law:

$$J = (9/8) (K \epsilon_0 \mu V^2 / d^3) \quad (3)$$

where V and d are the applied voltage and the thickness of the device, respectively. The free hole concentration can be expressed, with the Fermi energy E_f , as $h = H_{\text{HOMO}} \exp(-E_f/kT)$, where H_{HOMO} is the density of state of the highest occupied molecular orbital (HOMO) and the energy of HOMO is set at zero. The trapped hole concentration within a single discrete-trap approximation, $h_t = H_t / \{ 1 + \exp[(E_f - E_t)/kT] \}$, can be rewritten as

$$h_t = H_t / (1 + [H_{\text{HOMO}} \exp(-E_t/kT)] / h) \quad (4)$$

with H_t being the hole trap density and E_t the hole trap energy. In this expression, the trap degeneracy is assumed to one. The solution to Eqs. (1) and (2) using Eq. (4) with a low charge injection limit gives the I/V relationship for the discrete-trap charge limit (D-TCL) as

$$J \approx (9/8) [K \epsilon_0 \mu V^2 / (1 + \mathcal{G}^{-1}) d^3] \quad (5)$$

with

$$\mathcal{G} = (H_{\text{HOMO}} / H_t) \exp(-E_t/kT) \quad (6)$$